



This is a repository copy of *Modeling the human tibio-femoral joint using ex vivo determined compliance matrices.*

White Rose Research Online URL for this paper:
<https://eprints.whiterose.ac.uk/99263/>

Version: Accepted Version

Article:

Lamberto, G. orcid.org/0000-0001-7038-2655, Richard, V., Dumas, R. et al. (5 more authors) (2016) Modeling the human tibio-femoral joint using ex vivo determined compliance matrices. *Journal Of Biomechanical Engineering*, 138 (6). 061010. ISSN 0148-0731

<https://doi.org/10.1115/1.4033480>

Reuse

Items deposited in White Rose Research Online are protected by copyright, with all rights reserved unless indicated otherwise. They may be downloaded and/or printed for private study, or other acts as permitted by national copyright laws. The publisher or other rights holders may allow further reproduction and re-use of the full text version. This is indicated by the licence information on the White Rose Research Online record for the item.

Takedown

If you consider content in White Rose Research Online to be in breach of UK law, please notify us by emailing eprints@whiterose.ac.uk including the URL of the record and the reason for the withdrawal request.



eprints@whiterose.ac.uk
<https://eprints.whiterose.ac.uk/>

Modeling the human tibio-femoral joint using ex vivo determined compliance matrices

Giuliano Lamberto¹

Department of Movement, Human, and Health Sciences

Università degli Studi di Roma - Foro Italico

Piazza Lauro de Bosis 6

00194 Rome, Italy

Department of Mechanical Engineering and INSIGNEO Institute for *in silico* Medicine,

University of Sheffield,

Mappin Street,

Sheffield - S1 3JD, United Kingdom

e-mail: glamberto1@sheffield.ac.uk

Vincent Richard

Université de Lyon,

Université Claude Bernard Lyon 1, IFSTTAR, UMR_T9406

Laboratoire de Biomécanique et Mécanique des Chocs

Bron, France

e-mail: vincent.richard@univ-lyon1.fr

Raphaël Dumas

Université de Lyon,

Université Claude Bernard Lyon 1, IFSTTAR, UMR_T9406

Laboratoire de Biomécanique et Mécanique des Chocs

Bron, France

e-mail: raphael.dumas@ifsttar.fr

Pier Paolo Valentini

Department of Enterprise Engineering “Mario Lucertini”

Università degli Studi di Roma - Tor Vergata

Via del Politecnico, 1

00133 Rome, Italy

e-mail: valentini@ing.uniroma2.it

¹ Corresponding author at: Department of Mechanical Engineering, The University of Sheffield, INSIGNEO Institute for *in silico* medicine, Room C+ 13, C+ floor, The Pam Liversidge Building, Sir Frederick Mappin Building, Mappin Street, Sheffield - S1 3JD, UK. E-mail address: glamberto1@sheffield.ac.uk

Ettore Pennestri
Department of Enterprise Engineering "Mario Lucertini"
Università degli Studi di Roma - Tor Vergata
Via del Politecnico, 1
00133 Rome, Italy
e-mail: pennestri@mec.uniroma2.it
ASME Member

Tung-Wu Lu
Institute of Biomedical Engineering, and
Department of Orthopedic Surgery
National Taiwan University
No. 1, Section 4, Roosevelt Road
Taipei 106, Taiwan
e-mail: twlu@ntu.edu.tw

Valentina Camomilla
Department of Movement, Human, and Health Sciences
Università degli Studi di Roma - Foro Italico
Piazza Lauro de Bosis 6
00194 Rome, Italy
e-mail: valentina.camomilla@uniroma4.it

Aurelio Cappozzo
Department of Movement, Human, and Health Sciences
Università degli Studi di Roma - Foro Italico
Piazza Lauro de Bosis 6
00194 Rome, Italy
e-mail: aurelio.cappozzo@uniroma4.it

1 **ABSTRACT**

2 *Several approaches have been used to devise a model of the human tibio-femoral joint for*
3 *embedment in lower limb musculoskeletal models. However, no study has considered the use of cadaveric*
4 *6x6 compliance (or stiffness) matrices to model the tibio-femoral joint under normal or pathological*
5 *conditions. The aim of this paper is to present a method to determine the compliance matrix of an ex vivo*
6 *tibio-femoral joint for any given equilibrium pose. Experiments were carried out on a single ex vivo knee,*
7 *first intact and, then, with the anterior cruciate ligament (ACL) transected. Controlled linear and angular*
8 *displacements were imposed in single degree-of-freedom (DoF) tests to the specimen and resulting forces*
9 *and moments measured using an instrumented robotic arm. This was done starting from seven*
10 *equilibrium poses characterized by the following flexion angles: 0°, 15°, 30°, 45°, 60°, 75° and 90°. A*
11 *compliance matrix for each of the selected equilibrium poses and for both the intact and ACL deficient*
12 *specimen was calculated. The matrix, embedding the experimental load-displacement relationship of the*
13 *examined DoFs, was calculated using a linear least squares inversion based on a QR decomposition,*
14 *assuming symmetric and positive-defined matrices. Single compliance matrix terms were in agreement*
15 *with the literature. Results showed an overall increase of the compliance matrix terms due to the ACL*
16 *transection (2.6 ratio for rotational terms at full extension) confirming its role in the joint stabilization.*
17 *Validation experiments were carried out by performing a Lachman test (the tibia is pulled forward) under*
18 *load control on both the intact and ACL-deficient knee and assessing the difference (error) between*
19 *measured linear and angular displacements and those estimated using the appropriate compliance matrix.*
20 *This error increased non-linearly with respect to the values of the load. In particular, when an incremental*
21 *posterior-anterior force up to 6 N was applied to the tibia of the intact specimen, the errors on the*
22 *estimated linear and angular displacements were up to 0.6 mm and 1.5°, while for a force up to 18 N the*
23 *errors were 1.5 mm and 10.5°, respectively.*

24 *In conclusion, the method used in this study may be a viable alternative to characterize the tibio-*
25 *femoral load-dependent behavior in several applications.*

27 **INTRODUCTION**

28 Biomechanical modeling of the knee joint has been the object of several studies
29 in the last 30 years [1–12] with the aim of better understanding the passive joint
30 behavior and estimate the joint contact and ligament forces during motor tasks under
31 physiological and pathological conditions. To address these objectives, comprehensive
32 finite element or multi-body models [13–18] have been developed and, in some cases,
33 validated against *ex vivo* data. Due to numerical issues, knee models in general rely on
34 kinematic constraints (i.e. degree-of-freedom (DoF) restraints) [8,19], which may include
35 ligaments with infinite stiffness and/or passive joint moments [20,21]. The passive joint
36 moments are linear or exponential functions of the joint angles and are introduced in
37 simulations mainly with the aim of preventing exceedingly large joint amplitudes. The
38 stiffness values, embedded in these curves, are not determined experimentally but
39 result from a tuning or calibration procedure and comply with numerical requirements
40 of the optimization approach. Another modeling approach, called “force dependent
41 kinematics”, has been recently proposed [22,23]. The idea is to optimize the estimate of
42 joint kinematics to ensure the static equilibrium of the joint according to a set of
43 stiffness values, again, resulting from a numerical procedure.

44 An alternative modeling approach would be to directly introduce a knee
45 compliance matrix (or its inverse named stiffness matrix) resulting from *ex vivo*
46 experiments into the musculoskeletal model. This matrix provides the joint

47 displacements as a function of the loads acting through the joint. Such approach has
48 been previously proposed for the intervertebral joints [24–27], but not for other joints.
49 One interesting property of the compliance matrix is that the extra-diagonal terms
50 describe the physiological couplings between the DoFs. In addition, pathological
51 conditions, such as ligament or meniscal tears, can be revealed by altered matrix terms.
52 Nevertheless, despite a general availability of robotic-manipulators [28], the knowledge
53 of the knee compliance matrix is rather limited. Indeed, investigations of the tibio-
54 femoral joint kinematics response to loading have been restricted either to few selected
55 directions or to a limited number of knee configurations (i.e., typically 0° of flexion). For
56 example, Markolf et al. [29] performed one of the most complete studies available,
57 analyzing the relationship between moments and adduction-abduction and internal-
58 external rotations, as well as force and linear displacement in the anterior-posterior
59 direction, at six different flexion angles. Eagar et al. [30] quantified the anterior-
60 posterior load-displacement behavior in both linear and non-linear regions at four
61 different flexion angles. Fox et al. [31] and Kanamori et al. [32] determined the *in situ*
62 forces in the posterior and anterior cruciate ligaments, respectively, in response to
63 different loading conditions and in more than one configuration (i.e. 0°, 15°, 30°, 60°,
64 90° of flexion). However, to the best of our knowledge, only Loch et al. [33] tried to
65 characterize the mechanical behavior of the passive structures that constrain the knee
66 joint using a compact 6x6 matrix, but that research was limited to a single knee

67 configuration (i.e., 0° of flexion). Moreover, the way the terms of the matrix were
68 derived from experimental data is not clearly stated.

69 The aim of this paper was to present a method to mathematically define and
70 experimentally determine a set of compliance matrices in different knee configurations.
71 The current study used a quasi-static approach by applying, through a robotic arm, small
72 displacements about a number of selected equilibrium poses of the knee [31,32]. The
73 load-displacement relationships were expressed by 6x6 symmetric compliance matrices.
74 Experiments were carried out on a cadaveric knee specimen, both intact and with the
75 anterior cruciate ligament (ACL) transected. In addition, a validation procedure was
76 implemented to test the ability of the compliance matrix to estimate linear and angular
77 displacements as caused by an arbitrary load.

78 **MATERIALS AND METHODS**

79 **Specimen preparation**

80 A single intact fresh-frozen human knee joint obtained from a 75 year old female
81 was tested. The specimen was a left leg derived from an amputation due to an acute
82 arterial occlusion. Ethical approval for the study was granted by the Institutional
83 Research Board of China Medical University Hospital (Taichung City, Taiwan). The knee
84 was kept frozen until the time of use. It was declared normal by the surgeon who
85 prepared it for the experiments. It was sectioned at the mid-shaft of the femur and tibia
86 and dissected down to the joint capsule and major ligaments. All the muscles, the

87 patella, and the patellar tendon were removed in order to mechanically characterize the
88 behavior of the tibio-femoral passive structures. The bones were mounted through
89 cement in two aluminum fixation supports to be connected to a Robot-based Joint
90 Testing System (RJTS) [34]. On the day of testing, the knee was thawed and pre-
91 conditioned [35]. After testing the intact knee, all the ACL bundles were surgically
92 transected and the experimental procedure repeated.

93 **Experimental apparatus and procedure**

94 The RJTS consists of an industrial robotic system (RV-20A, Mitsubishi Electric
95 Corporation, Japan) and a six-component load cell (Universal Force Sensor, Model PY6-
96 100, Bertec Corporation, USA) that was attached to the end effector of the robot for the
97 measurement of the three force and three moment components of the load (Figure 1A).
98 The robot was recently developed for applications in *ex vivo* biomechanical studies [34].
99 This testing device is capable of a hybrid position/load control using traditional and
100 innovative methods. Control methods were evaluated performing tests on a human
101 cadaveric knee both in translation along and in rotation about a selected axis, where
102 their convergence and their residual constraining load were compared against published
103 standard methods. The results, showing a repeat accuracy of 0.1 mm, suggested system
104 suitability for accurate and reliable testing of biological joints [34]. The sampling rate of
105 the acquisition was 10 samples per second.

106 A method to identify bony landmarks for the definition of femur and tibia
107 anatomical coordinated systems and therefore of the knee joint coordinate system (JCS)

108 was adapted from Fujie et al. [36] (Figure 1A). A calibration procedure was performed
109 using a pointer mounted on the end-effector of the robot. Using this pointer, the
110 position of the femoral insertion sites of the medial collateral ligament and the lateral
111 collateral ligament were identified in the global coordinate system. The centroid of the
112 femoral section was assumed as coincident with the geometrical center of the fixation
113 support, the position of which was determined before mounting the specimen. These
114 points were used to define the anatomical coordinate system of the femur (C_f) (details
115 in Figure 1B). The anatomical coordinate system of the tibia (C_t) was defined as
116 coincident with C_f at full extension. The forces and moments were recorded by the load
117 cell in the sensor coordinate system (C_s) (Figure 1A).

118 Flexion-extension (F-E), adduction-abduction (A-A), and internal-external (I-E)
119 rotations were defined as motions about the JCS axes (e1: z-axis of C_f , e2: floating axis,
120 e3: y-axis of C_t). Medial-lateral (M-L), anterior-posterior (A-P), and proximal-distal (P-D)
121 linear displacements were characterized as motions along these axes. A sign inversion
122 was used to report positive values for the flexion angles, otherwise negative by
123 convention. Measured loads were represented in the JCS using a Jacobian matrix [37].

124 A set of pre-determined F-E angles were used to determine the compliance
125 matrices of the intact knee: 0°, 15°, 30°, 45°, 60°, 75° and 90°. For each F-E angle, the
126 neutral pose, i.e. the A-A and I-E rotations, and M-L, A-P and P-D displacements, was
127 determined so that the measured joint moments and forces were minimal [37]. The
128 same neutral poses were later used for the ACL-deficient knee experiment. Constrained

129 control was then used to perform single DoF tests [34]. These tests were defined by the
 130 application of the following procedure: starting from the neutral pose, linear or angular
 131 displacement increments (at rates of 0.93 mm/s and 0.97 °/s) were applied one at a
 132 time along and about each single DoF, under moment and force limitations to avoid any
 133 damage to the soft tissues. The force limitations, adopted both for the intact and ACL-
 134 deficient knee, were 100 N along A-P and P-D, and 80 N along L-M as similarly applied in
 135 [38]. Limitations of moments were conservatively set at 25% of those used in [29,39],
 136 and were 2.5 Nm for A-A, and 1 Nm for I-E.

137 To evaluate the prediction capability of the compliance matrix, a Lachman test
 138 was simulated. With the knee flexed at 30°, a force, linearly increasing in time, was
 139 applied to the tibia along the A-P axis, under the force limitation mentioned previously.
 140 The whole experimental procedure is summarized in Table 1.

141 **Post-processing procedure**

142 The post-processing procedure was based on the procedure proposed by Stokes
 143 et al. [40] and adapted to the experimental data of the present study.

144 The compliance matrix $[C]$ is 6x6 symmetric:

$$[C]\{F - F_0\} = \{X - X_0\} \quad (1)$$

145 where $\{X\}$ is a 6x1 generalized displacement vector of the A-P, P-D and M-L
 146 displacements followed by the A-A, I-E, and F-E rotations and $\{F\}$ is a 6x1 load vector of
 147 the corresponding forces and moments. $\{X_0\}$ and $\{F_0\}$ are the same 6x1 vectors
 148 obtained at the neutral poses of the knee. The generic 6x6 symmetric compliance matrix

149 [C] has 21 independent compliance terms (6 translational, 6 rotational, and 9 coupling
150 terms), $\{c\}$, that can be obtained by rearranging Eq. 1 into the standard least squares
151 inversion form:

$$[L]\{c\} = \{X - X_0\} \quad (2)$$

152 where $[L]$ is a 6x21 matrix based on the six terms of $\{F - F_0\}$ (the incremental load
153 vectors) and $\{c\}$ is a 21x1 vector of the 21 independent compliance matrix terms. This
154 vector $\{c\}$ was obtained through a least squares inversion using, for each F-E angle, the
155 3D displacements and loads obtained from all the incremental displacements applied
156 about each single DoF. In this way, it is not the 6*6 matrix terms that were computed
157 but the 21 independent terms directly. Thus, the 9 coupling terms have not been
158 averaged to make the matrix symmetric, as is performed classically in the literature [41].
159 Compliance terms were set as unknown to be determined with respect to the stiffness
160 terms. This approach prevented proportional vectors in the coefficient matrix of the
161 standard least squares form (Eq. 2). In fact, setting stiffness terms as unknown would
162 have filled the coefficient matrix with the proportional imposed linear increments of the
163 single DoF tests, introducing a rank-deficiency in the computation. In addition, a QR
164 decomposition was used to avoid numerical instability [42] and each matrix was
165 constrained to be positive defined. Re-sampling using cubic spline interpolation was
166 performed since the data has different frame numbers, according to the different
167 moment and force limitations imposed. Ultimately, only the first fifteen frames were
168 considered to ensure a certain range of linearity around the neutral pose and, at the

169 same time, to consider the contribution of each single DoF test to the overall matrix.
170 Concerning the latter aspect, at least ten frames from each single DoF test were
171 assumed to be representative in the overall matrix.

172 **Validation**

173 For the purpose of validation, the compliance matrices computed at 30° of F-E
174 with both intact and ACL-deficient knee were used to predict the A-P, P-D and M-L
175 displacements and A-A, I-E and F-E rotations using Eq. 1 and the forces and moments
176 measured during the simulated Lachman test. The absolute errors between calculated
177 and measured linear and angular displacements were computed.

178 **RESULTS**

179 The compliance matrices for the intact and the ACL-deficient knee are displayed
180 at 0° and 30° of F-E in Table 2 and Table 3, respectively. The matrices for the other
181 neutral poses can be found in the Appendix.

182 The vast majority of the calculated compliance terms were modified by the ACL
183 transection. As expected, the values of the compliance terms increased after the ACL
184 dissection when compared to their values for the intact knee structures. For instance, at
185 full extension, the incremental ratios between the sum of the compliance terms of each
186 subgroup before and after the dissection were 1.51, 2.60, and 0.83 for the translational,
187 rotational, and coupling terms, respectively. This behavior accounts for the fundamental
188 role of the ACL in preventing extreme tibio-femoral displacements when a force is
189 applied. In addition, non-negligible coupling terms depending to the particular flexion

190 angle were found. This highlights the fact that it is important to estimate the compliance
191 matrix in more than one configuration.

192 The validation tests performed using the compliance matrices obtained at 30° of
193 F-E for the intact and ACL-deficient knee (Table 3), are illustrated in Figure 2 and Figure
194 3, respectively. The following quantities are depicted as a function of time: the absolute
195 errors (panels A and B) and the values of the three linear and three angular
196 displacement components (panels C and D) computed through the compliance matrix
197 (Eq. 1) using the forces and moments (panels E and F) recorded during the simulated
198 Lachman test. Coherent results were achieved both for the intact and the ACL-deficient
199 knees at the beginning of the validation experiments, that is, when small loads were
200 applied in proximity of the neutral pose. However, at a later stage of the experiment,
201 absolute errors were found to increase. In particular, for controlled forces below 6 N
202 and 3 N for the intact and the ACL-deficient knee (0-0.5 s of testing), the maximum
203 absolute errors were 0.58 mm, 0.21 mm and 1.49°, 0.57° for the linear and angular
204 displacements, respectively. For controlled forces below 11 N and 8 N (0.6-1 s of
205 testing), the errors were 1.14 mm, 0.83 mm, and 4.60°, 2.95°, respectively and increased
206 to 1.49 mm, 2.35 mm, and 10.36°, 3.36° when forces reached 18 N and 15 N (1.1-1.5 s of
207 testing).

208 **DISCUSSION**

209 In the present study, the mathematical definition and experimental
210 determination of compliance matrices in different knee configurations was developed.

211 The mathematical definition is based on a compliance matrix which led to a higher
212 number of independent rows in the calculation process with respect to the stiffness
213 matrix. The compliance terms are computed through a least squares inversion based on
214 QR decomposition, and the positive definition of all the matrices computed was ensured
215 for a possible use as stiffness matrices. The experimental determination was performed,
216 using a previously described Robot-based Joint Testing System [34], in different knee
217 configurations on both an intact and ACL-deficient knee. The compliance of the
218 knee/robot complex was computed under the assumption that the stiffness of the robot
219 components is much higher than the knee surrounding tissues and, therefore, can be
220 attributed exclusively to the knee [31,39].

221 Validation tests of the compliance matrix determined at 30° of F-E (Lachman
222 test) confirmed the ability to predict the A-P, P-D and M-L displacements and A-A, I-E
223 and F-E rotations for given loads applied on the JCS axes. The maximum absolute error
224 between predicted and measured knee linear and angular displacements increased non-
225 linearly with respect to the values of the applied load, both for the intact and the ACL-
226 deficient knee. As a result of the deviations from the starting neutral pose (more than
227 1mm and/or 1°) occurring when a force higher than 10 N in the A-P direction was
228 applied, caution should be exercised in using the compliance matrix when high
229 loads/displacements occur. This is also why only the first fifteen frames of the linear and
230 angular increments of each single DoF test were used for the determination of the
231 compliance terms. Some preliminary tests revealed that for a larger number of frames

232 the residual of the least squares inversion was higher. The cited number of frames was
233 selected as a good trade-off between a warranted linearity of load-displacement curves
234 and an ensured contribution of each single DoF test to the overall matrix.

235 Although no other study performed the determination of a set of compliance
236 matrices in different knee configurations, the current results can be compared with
237 studies estimating specific terms of the compliance matrix obtained at 0° of F-E (Table
238 2). The obtained compliance terms in the first row and first column compared well with
239 those obtained in *Markolf's* work [29], during an A-P stability test: the ratio after and
240 before ACL-section was 0.29 in the current study and 0.31 in [29]. Similarly, in A-P
241 direction the first diagonal term (about 0.08 mm/N) was in the range obtained by Eagar
242 et al. [30] who tested seven intact knee specimens (between 0.02 and 0.17 mm/N).
243 However, in that study, the neutral path of flexion-extension at the knee was not
244 defined and, as a result, no other knee configuration can be compared with the current
245 study. Ultimately, comparing our results with the stiffness matrix calculated by Loch et
246 al. [33] some similarities and differences could be found. In particular, the first two
247 translation compliance terms have the same order of magnitude as in [33], during six
248 independent displacement tests. Conversely, in our compliance matrix the third
249 translation compliance term and the rotational terms are two or more orders of
250 magnitude bigger than in [33]. These discrepancies can be attributed to the difference in
251 the neutral pose at full extension since a preload was applied in [33].

252 The current study is based on one important assumption, which may limit the
253 domain of application of the obtained results. In accordance with the literature [33], it is
254 assumed that, for small linear or angular displacements relative to the overall dimension
255 of the knee bones, the load-displacement behavior is linear, i.e. the compliance matrices
256 are symmetric. A second limiting factor in the application of current results is narrowing
257 the focus only on the passive structures that constrain the human knee, therefore
258 excluding muscular tendinous tissues, patella and patellar tendon as possible
259 contributors to the stability or load-bearing forces. Thirdly, this study focused on only
260 one knee specimen as other studies did [43,44]. The experimental procedure was
261 extremely time-consuming and the focus was more on determining the compliance
262 matrices in different knee configurations than testing multiple specimens.

263 Despite the limitations mentioned, the proposed set of compliance matrices can
264 be used to model the knee joint for its effective embedment in a musculoskeletal model
265 of the lower limb with low computational cost. The stiffness matrix (i.e., inverse of the
266 compliance matrix) of the intervertebral joints has been widely used in multi-body
267 models [24,26,45,46]. The study proposed here for the knee joint could be the first step
268 on the path covered previously for the spine. For that, the definition of the neutral pose
269 is of paramount importance to compute the joint passive moments and the elastic
270 energy. As shown in the compliance matrix validation performed in the current study,
271 this joint modeling is valid only near the neutral poses. Therefore, the definition of a set

272 of compliance matrices at different knee configurations (0°, 15°, 30°, 45°, 60°, 75° and
273 90° in this work) is of paramount importance.

274 The introduction of these matrices, or of corresponding stiffness matrices, into
275 musculoskeletal models of the lower limb will be the next step to provide alternatives
276 for femur and tibia pose estimation during movement using stereophotogrammetry and
277 skin markers and the so-named multi-body optimization [47]. Such “compliant”
278 constraints may provide better results than infinitely stiff constraints, like spherical or
279 hinge joints or parallel mechanisms [48–50]. The use of the matrices determined with
280 the ACL-deficient knee open the way for defining pathological constraints.

281 In conclusion, the method proposed in this study may be a viable alternative to
282 characterize the tibio-femoral load-dependent behavior in several applications. This
283 contribution might have implications on a new generation of lower limb musculoskeletal
284 models.

285

286 **ACKNOWLEDGMENT**

287 The authors wish to thank Li-De Chang, Tchung Whao, Mei-Ying Kuo, Elena
288 Bergamini and Valerio Rossi for providing technical and logistical support during and
289 after the experimental tests of this research.

290

291

292

293 **FUNDING**

294 This study was supported by a grant provided by the Università di Roma “Foro
295 Italico”, call 2012, named “A piecewise elastic model of the human tibiofemoral joint: a
296 feasibility study”.

297 **APPENDIX**

298 Compliance matrices at 15°, 45°, 60°, 75° and 90° of F-E for both intact and ACL-
299 sectioned knee tested are shown in Table 4 and Table 5.

REFERENCES

- 300 [1] Yamaguchi, G. T., and Zajac, F. E., 1989, "A planar model of the knee joint to
301 characterize the knee extensor mechanism," *J. Biomech.*, **22**(1), pp. 1–10.
- 302 [2] Beynnon, B., Yu, J., Huston, D., Fleming, B., Johnson, R., Haugh, L., and Pope, M.
303 H., 1996, "A sagittal plane model of the knee and cruciate ligaments with
304 application of a sensitivity analysis.," *J. Biomech. Eng.*, **118**(2), pp. 227–39.
- 305 [3] Hu, C.-C., Lu, T.-W., and Chen, S.-C., 2013, "Influence of model complexity and
306 problem formulation on the forces in the knee calculated using optimization
307 methods.," *Biomed. Eng. Online*, **12**(1), p. 20.
- 308 [4] Fernandez, J. W., and Pandy, M. G., 2006, "Integrating modelling and
309 experiments to assess dynamic musculoskeletal function in humans.," *Exp.*
310 *Physiol.*, **91**(2), pp. 371–82.
- 311 [5] Yang, N. H., Canavan, P. K., Nayeb-Hashemi, H., Najafi, B., and Vaziri, A., 2010,
312 "Protocol for constructing subject-specific biomechanical models of knee joint.,"
313 *Comput. Methods Biomech. Biomed. Engin.*, **13**(5), pp. 589–603.
- 314 [6] Halloran, J. P., Petrella, A. J., and Rullkoetter, P. J., 2005, "Explicit finite element
315 modeling of total knee replacement mechanics.," *J. Biomech.*, **38**(2), pp. 323–31.
- 316 [7] Ribeiro, A., Rasmussen, J., Flores, P., and Silva, L. F., 2012, "Modeling of the
317 condyle elements within a biomechanical knee model," *Multibody Syst. Dyn.*,
318 **28**(1-2), pp. 181–197.
- 319 [8] Arnold, E. M., Ward, S. R., Lieber, R. L., and Delp, S. L., 2010, "A model of the
320 lower limb for analysis of human movement.," *Ann. Biomed. Eng.*, **38**(2), pp. 269–
321 79.
- 322 [9] Sancisi, N., and Parenti-Castelli, V., 2011, "A sequentially-defined stiffness model
323 of the knee," *Mech. Mach. Theory*, **46**(12), pp. 1920–1928.
- 324 [10] Baldwin, M. a, Clary, C. W., Fitzpatrick, C. K., Deacy, J. S., Maletsky, L. P., and
325 Rullkoetter, P. J., 2012, "Dynamic finite element knee simulation for evaluation of
326 knee replacement mechanics.," *J. Biomech.*, **45**(3), pp. 474–83.
- 327 [11] Shelburne, K. B., Torry, M. R., and Pandy, M. G., 2005, "Muscle, Ligament, and
328 Joint-Contact Forces at the Knee during Walking," *Med. Sci. Sport. Exerc.*, **37**(11),
329 pp. 1948–1956.
- 330 [12] Moissenet, F., Chèze, L., and Dumas, R., 2014, "A 3D lower limb musculoskeletal
331 model for simultaneous estimation of musculo-tendon, joint contact, ligament
332 and bone forces during gait.," *J. Biomech.*, **47**(1), pp. 50–8.
- 333 [13] Bendjaballah, M. Z., Shirazi-Adl, a., and Zukor, D. J., 1998, "Biomechanical
334 response of the passive human knee joint under anterior-posterior forces.," *Clin.*
335 *Biomech. (Bristol, Avon)*, **13**(8), pp. 625–633.

- 336 [14] Donahue, T. L. H., Hull, M. L., Rashid, M. M., and Jacobs, C. R., 2002, "A finite
337 element model of the human knee joint for the study of tibio-femoral contact.," J.
338 Biomech. Eng., **124**(3), pp. 273–80.
- 339 [15] Peña, E., Calvo, B., Martínez, M. a, and Doblaré, M., 2006, "A three-dimensional
340 finite element analysis of the combined behavior of ligaments and menisci in the
341 healthy human knee joint.," J. Biomech., **39**(9), pp. 1686–701.
- 342 [16] Li, G., Gil, J., Kanamori, a, and Woo, S. L., 1999, "A validated three-dimensional
343 computational model of a human knee joint.," J. Biomech. Eng., **121**(6), pp. 657–
344 62.
- 345 [17] Guess, T. M., Thiagarajan, G., Kia, M., and Mishra, M., 2010, "A subject specific
346 multibody model of the knee with menisci.," Med. Eng. Phys., **32**(5), pp. 505–15.
- 347 [18] Kazemi, M., Dabiri, Y., and Li, L. P., 2013, "Recent advances in computational
348 mechanics of the human knee joint.," Comput. Math. Methods Med., **2013**, p.
349 718423.
- 350 [19] Xu, H., Bloswick, D., and Merryweather, A., 2014, "An improved OpenSim gait
351 model with multiple degrees of freedom knee joint and knee ligaments.,"
352 Comput. Methods Biomech. Biomed. Engin., **18**(11), pp. 1217–1224.
- 353 [20] Al Nazer, R., Rantalainen, T., Heinonen, a, Sievänen, H., and Mikkola, a, 2008,
354 "Flexible multibody simulation approach in the analysis of tibial strain during
355 walking.," J. Biomech., **41**(5), pp. 1036–43.
- 356 [21] Anderson, F. C., and Pandy, M. G., 2001, "Dynamic Optimization of Human
357 Walking," J. Biomech. Eng., **123**(5), pp. 381–390.
- 358 [22] Andersen, M., Damsgaard, M., and Rasmussen, J., 2011, "Force-dependent
359 kinematics: a new analysis method for non-conforming joints," 13th International
360 Symposium on Computer Simulation in Biomechanics, pp. 1–2.
- 361 [23] Andersen, M., and Rasmussen, J., 2011, "Total knee replacement musculoskeletal
362 model using a novel simulation method for non-conforming joints," Proceedings
363 of the International Society of Biomechanics of the International Society of
364 Biomechanics, pp. 1–2.
- 365 [24] Christophy, M., Faruk Senan, N. A., Lotz, J. C., and O'Reilly, O. M., 2012, "A
366 Musculoskeletal model for the lumbar spine," Biomech. Model. Mechanobiol.,
367 **11**(1), pp. 19–34.
- 368 [25] Koell, P., Cheze, L., and Dumas, R., 2010, "Prediction of internal spine
369 configuration from external measurements using a multi-body model of the
370 spine," Comput. Methods Biomech. Biomed. Engin., **13**(sup1), pp. 79–80.
- 371 [26] Petit, Y., Aubin, C. E., and Labelle, H., 2004, "Patient-specific mechanical
372 properties of a flexible multi-body model of the scoliotic spine," Med. Biol. Eng.
373 Comput., **42**(1), pp. 55–60.

- 374 [27] Marin, F., Hoang, N., Aufaure, P., and Ho Ba Tho, M. C., 2010, "In vivo
375 intersegmental motion of the cervical spine using an inverse kinematics
376 procedure," *Clin. Biomech.*, **25**(5), pp. 389–396.
- 377 [28] Fujie, H., Mabuchi, K., and Woo, S., 1993, "The use of robotics technology to
378 study human joint kinematics: a new methodology.," *J. Biomech. Eng.*, **115**(3), pp.
379 211–7.
- 380 [29] Markolf KL, Mensch, J., and Amstutz, H., 1976, "Stiffness and laxity of the knee -
381 the contributions of the supporting structures.," *J. Bone Joint Surg. Am.*, **58**(5),
382 pp. 583–94.
- 383 [30] Eagar, P., Hull, M. L., and Howell, S. M., 2001, "A method for quantifying the
384 anterior load-displacement behavior of the human knee in both the low and high
385 stiffness regions.," *J. Biomech.*, **34**(12), pp. 1655–60.
- 386 [31] Fox, R. J., Harner, C. D., Sakane, M., Carlin, G. J., and Woo, S. L., 1998,
387 "Determination of the in situ forces in the human posterior cruciate ligament
388 using robotic technology. A cadaveric study.," *Am. J. Sports Med.*, **26**(3), pp. 395–
389 401.
- 390 [32] Kanamori, A., Woo, S. L., Ma, C. B., Zeminski, J., Rudy, T. W., Li, G., and Livesay, G.
391 a, 2000, "The forces in the anterior cruciate ligament and knee kinematics during
392 a simulated pivot shift test: A human cadaveric study using robotic technology.,"
393 *Arthroscopy*, **16**(6), pp. 633–9.
- 394 [33] Loch, D. a, Luo, Z. P., Lewis, J. L., and Stewart, N. J., 1992, "A theoretical model of
395 the knee and ACL: theory and experimental verification.," *J. Biomech.*, **25**(1), pp.
396 81–90.
- 397 [34] Hsieh, H.-J., Hu, C.-C., Lu, T.-W., Kuo, M.-Y., Kuo, C.-C., and Hsu, H.-C., "Evaluation
398 of Three Force-Position Hybrid Control Methods for a Robot-Based Biological
399 Joint Testing System," *Submitt. to Biomed. Eng. Online*.
- 400 [35] Most, E., Axe, J., Rubash, H., and Li, G., 2004, "Sensitivity of the knee joint
401 kinematics calculation to selection of flexion axes.," *J. Biomech.*, **37**(11), pp.
402 1743–8.
- 403 [36] Fujie, H., Sekito, T., and Orita, A., 2004, "A novel robotic system for joint
404 biomechanical tests: application to the human knee joint.," *J. Biomech. Eng.*,
405 **126**(1), pp. 54–61.
- 406 [37] Fujie, H., Livesay, G., Fujita, M., and Woo, S., 1996, "Forces and moments in six-
407 DOF at the human knee joint: mathematical description for control," *J. Biomech.*,
408 **29**(12), pp. 1577–1585.
- 409 [38] Grood, E., 1988, "Limits of movement in the human knee. Effect of sectioning the
410 posterior cruciate ligament and posterolateral structures," *J Bone Jt. Surg Am*, pp.
411 88–97.

- 412 [39] Zantop, T., Herbort, M., Raschke, M. J., Fu, F. H., and Petersen, W., 2007, "The
413 role of the anteromedial and posterolateral bundles of the anterior cruciate
414 ligament in anterior tibial translation and internal rotation.," *Am. J. Sports Med.*,
415 **35**(2), pp. 223–7.
- 416 [40] Stokes, I. a, Gardner-Morse, M., Churchill, D., and Laible, J. P., 2002,
417 "Measurement of a spinal motion segment stiffness matrix.," *J. Biomech.*, **35**(4),
418 pp. 517–21.
- 419 [41] Gardner-Morse, M. G., and Stokes, I. a. F., 2004, "Structural behavior of human
420 lumbar spinal motion segments," *J. Biomech.*, **37**(2), pp. 205–212.
- 421 [42] Pennestrì, E., and Cheli, F., 2006, *Cinematica e dinamica dei sistemi multibody* (in
422 italian), vol.1, Casa Editrice Ambrosiana, Milano, Italy.
- 423 [43] Guess, T. M., Liu, H., Bhashyam, S., and Thiagarajan, G., 2011, "A multibody knee
424 model with discrete cartilage prediction of tibio-femoral contact mechanics.,"
425 *Comput. Methods Biomech. Biomed. Engin.*, **16**(3), pp. 256–70.
- 426 [44] Mommersteeg, T. J., Huiskes, R., Blankevoort, L., Kooloos, J. G., and Kauer, J. M.,
427 1997, "An inverse dynamics modeling approach to determine the restraining
428 function of human knee ligament bundles.," *J. Biomech.*, **30**(2), pp. 139–46.
- 429 [45] Christophy, M., Curtin, M., Faruk Senan, N. A., Lotz, J. C., and O'Reilly, O. M.,
430 2013, "On the modeling of the intervertebral joint in multibody models for the
431 spine," *Multibody Syst. Dyn.*, **30**, pp. 413–432.
- 432 [46] Kim, K., Kim, Y. H., and Lee, S., 2012, "General computational model for human
433 musculoskeletal system of spine," *J. Appl. Math.*, **2012**, pp. 1–8.
- 434 [47] Lu, T.-W., and O'Connor, J. J., 1999, "Bone position estimation from skin marker
435 co-ordinates using global optimisation with joint constraints," *J. Biomech.*, **32**(2),
436 pp. 129–134.
- 437 [48] Mokhtarzadeh, H., Perraton, L., Fok, L., Muñoz, M. A., Clark, R., Pivonka, P., and
438 Bryant, A. L., 2014, "A comparison of optimisation methods and knee joint
439 degrees of freedom on muscle force predictions during single-leg hop landings.,"
440 *J. Biomech.*, **47**(12), pp. 2863–2868.
- 441 [49] Di Gregorio, R., and Parenti-Castelli, V., 2003, "A Spatial Mechanism With Higher
442 Pairs for Modelling the Human Knee Joint," *J. Biomech. Eng.*, **125**(2), pp. 232–7.
- 443 [50] Ottoboni A, Parenti-Castelli V, Sancisi N, Belvedere C, L. A., 2010, "Articular
444 surface approximation in equivalent spatial parallel mechanism models of the
445 human knee joint: an experiment-based assessment.," *Proc Inst Mech Eng H*.
446

Figure Captions List

- Fig. 1 A) A schematic representation of the Robot-based Joint Testing System (RJTS) and the reference systems used are provided: G is the global coordinate system; C_s is the coordinate system of the load cell (LC) and C_f is the anatomical coordinate system of the femur. B) C_f was defined as follows: the origin was the midpoint between the medial collateral ligament (MCL) and lateral collateral ligament (LCL) insertions; the z-axis was made to pass through LCL and MCL (transepicondylar axis) and pointed towards the latter point. The y axis was defined as lying on the plane defined by LCL, MCL, and the centroid of the bone section (frontal plane) and perpendicular to the z axis pointing toward the proximal part of the bone. Finally, the x-axis was defined to be perpendicular to both the y- and the z-axes and oriented to generate a right-handed frame.
- Fig. 2 The absolute error for the intact knee between displacements (A) and rotations (B) measured and computed with the compliance matrix at 30° of F-E is displayed. The values of A-P, P-D and M-L computed displacements (C) and measured forces (E), of A-A, I-E and F-E rotations (D) and moments (F) are also illustrated.
- Fig. 3 Compliance matrix validation of the ACL-deficient knee. See Figure 2 for the explanation.

Table Caption List

- Table 1 The experimental procedure for the compliance matrices calculation and validation is summarized in a chronological order
- Table 2 Compliance matrix computed at 0° of F-E. Units of measurements are N, mm and rad. All the compliance matrix terms have to be scaled down by a factor of 10^{-5} . In this and the following tables, F_x , F_y , F_z , M_x , M_y , M_z refer to the force and moment components, respectively, and T_x , T_y , T_z , R_x , R_y , R_z to the linear displacement components and the rotations, respectively.
- Table 3 Compliance matrix computed at 30° of F-E. Units of measurements are N, mm and rad. All the compliance matrix terms have to be scaled down by a factor of 10^{-5} .
- Table 4 Compliance matrix computed at 15° and 45° of F-E. Units of measurements are N, mm and rad. All the compliance matrix terms have to be scaled down by a factor of 10^{-5} .
- Table 5 Compliance matrix computed at 60°, 75° and 90° of F-E. Units of measurements are N, mm and rad. All the compliance matrix terms have to be scaled down by a factor of 10^{-5} .

Figure 1

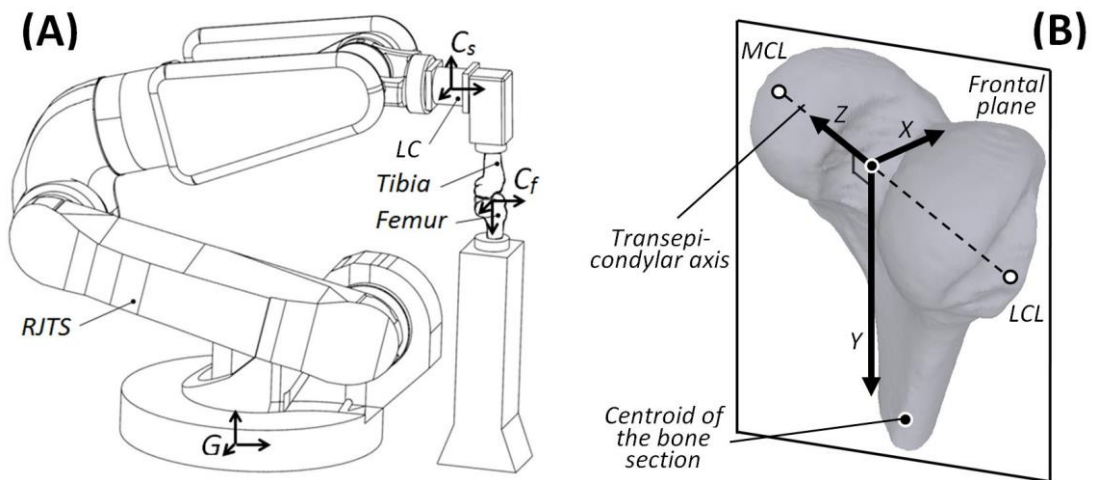


Figure 2

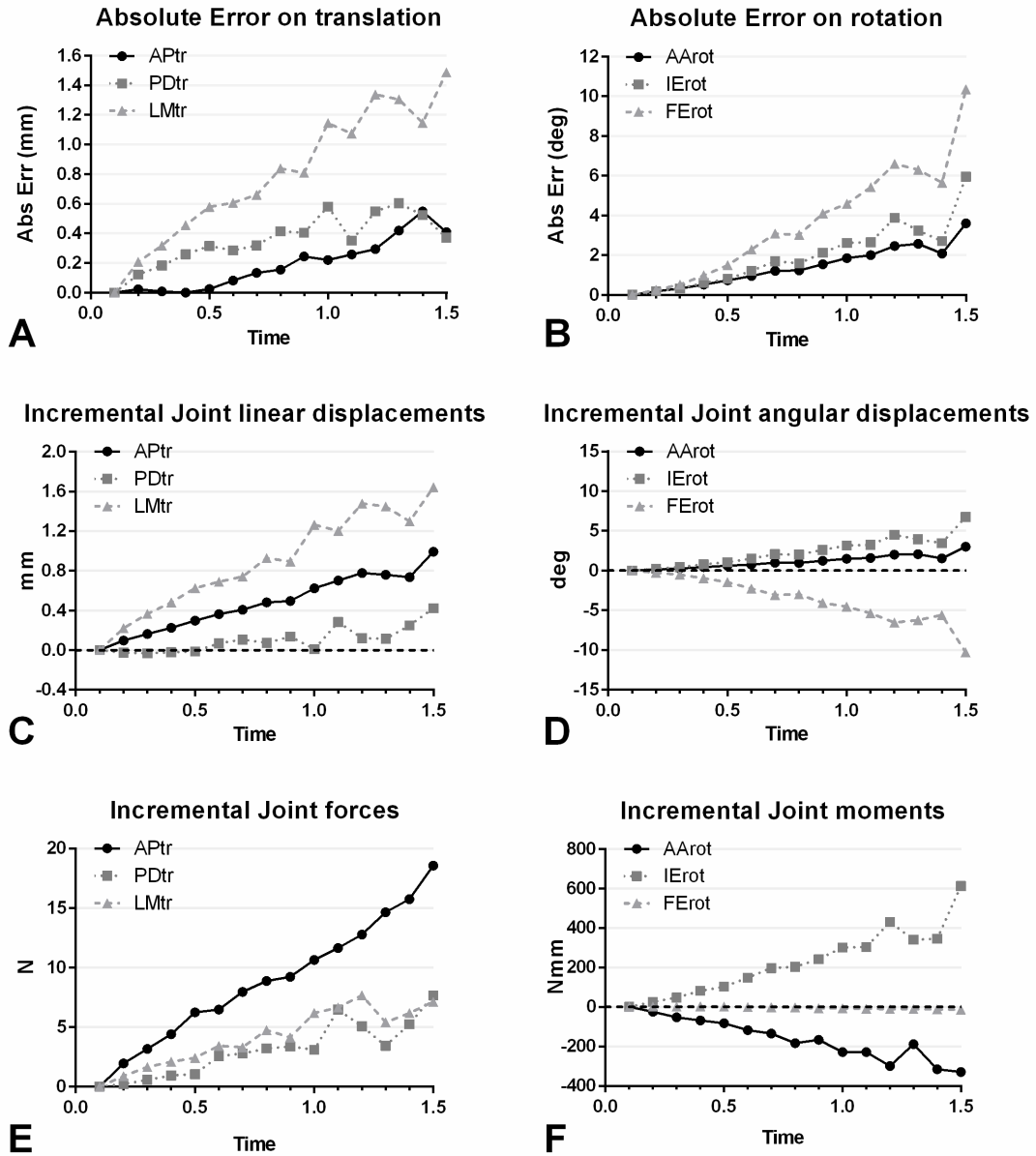


Figure 3

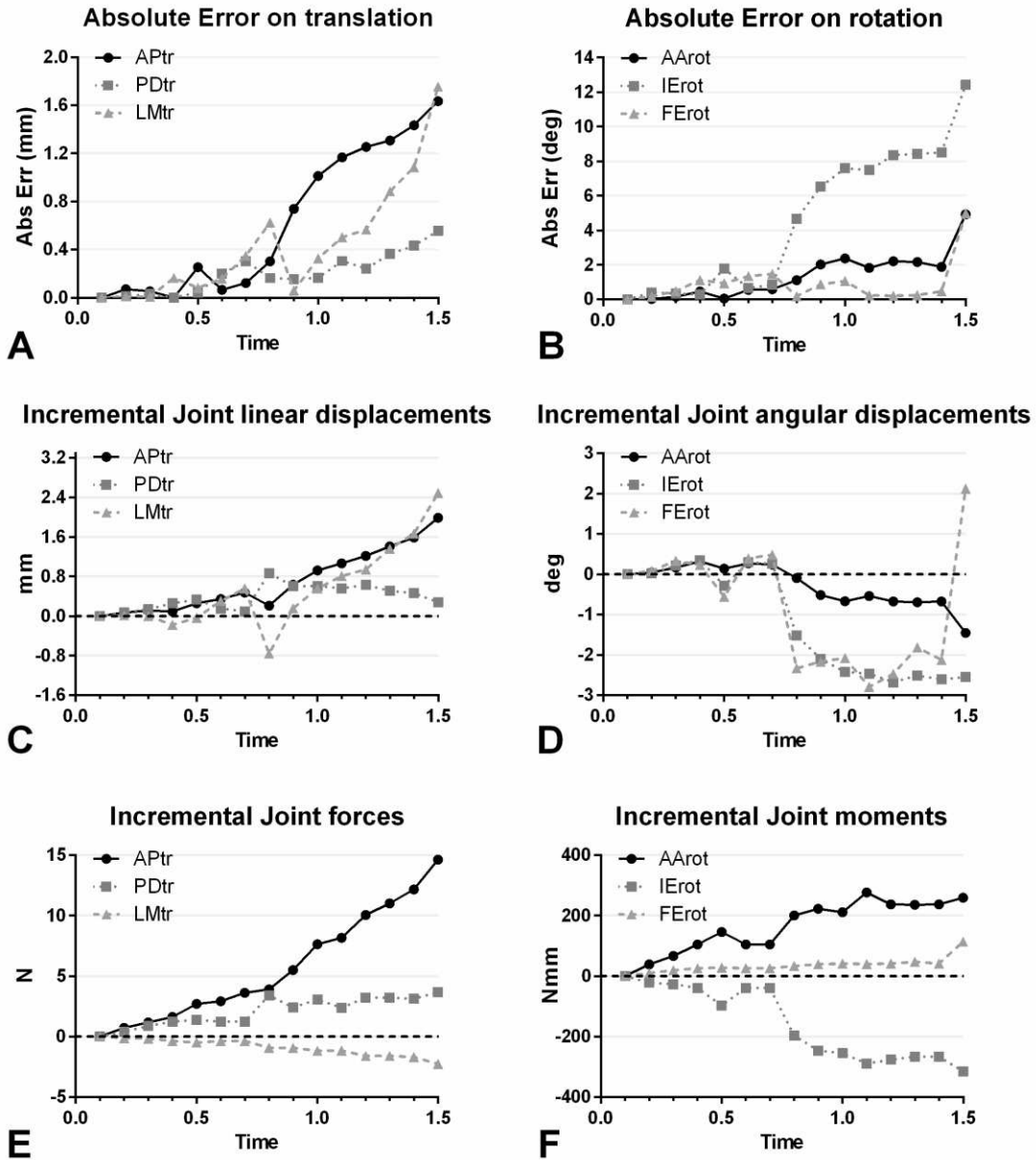


Table 1

Status of Knee	Knee F-E angle	Procedure steps	Robot Control	Compliance matrix calculation	Compliance matrix validation
Intact knee	0°, 15°, 30°, 45°, 60°, 75° and 90°	Determination of neutral pose of the knee	Hybrid control	✓	
		Single DoF tests	Constrained Control	✓	
	30°	Lachman test	Force control		✓
ACL-deficient knee	0°, 15°, 30°, 45°, 60°, 75° and 90°	Single DoF tests	Constrained Control	✓	
		30°	Lachman test	Force control	

Table 2

Status of knee	F_x	F_y	F_z	M_x	M_y	M_z	
intact	8483.0	-3601.3	1653.0	24.7	113.1	185.0	T_x
ACL cut	29173.0	-12305.8	-11451.1	104.8	-40.8	496.7	
intact		5575.4	-561.1	-1.9	-43.4	-134.7	T_y
ACL cut		14879.4	1225.2	59.2	15.0	-362.8	
intact			15712.5	28.0	279.9	-135.9	T_z
ACL cut			24440.1	-153.7	-66.0	-365.2	
intact				3.4	2.7	1.3	R_x
ACL cut				8.0	-1.3	-0.6	
intact		Symmetric			11.7	2.5	R_y
ACL cut					1.1	-0.8	
intact						12.7	R_z
ACL cut						22.0	

Table 3

Status of knee	F_x	F_y	F_z	M_x	M_y	M_z	
intact	2991.3	572.9	5793.4	92.5	42.1	-180.0	T_x
ACL cut	21321.8	-5513.2	27461.0	0.1	-332.5	-286.9	
intact		8559.8	-5852.4	-7.6	1.6	-312.3	T_y
ACL cut		17246.3	-24766.5	89.5	26.4	-258.2	
intact			16999.8	190.3	68.3	-56.0	T_z
ACL cut			76015.9	-217.6	-46.0	800.0	
intact				9.8	8.5	-18.4	R_x
ACL cut				33.9	39.1	-60.7	
intact		Symmetric			21.2	-26.3	R_y
ACL cut					62.9	-51.9	
intact						126.7	R_z
ACL cut						133.2	

Table 4

15° of F-E							
Status of knee	F _x	F _y	F _z	M _x	M _y	M _z	
Intact	15023.3	-14374.5	26922.1	-84.1	300.0	56.8	T _x
ACL cut	44335.6	-313.0	-2912.9	-19.7	-808.2	-797.4	
Intact		28838.7	-4517.2	293.0	128.1	-165.0	T _y
ACL cut		13218.2	-6324.4	140.5	-135.7	-713.0	
intact			96628.6	-175.2	-1065.2	108.3	T _z
ACL cut			13028.0	-134.9	14.7	-227.9	
intact				47.1	34.2	-16.6	R _x
ACL cut		Symmetric		4.9	1.5	-4.6	
intact					279.4	-13.7	R _y
ACL cut					21.9	26.3	
intact						26.5	R _z
ACL cut						95.1	

45° of F-E							
Status of knee	F _x	F _y	F _z	M _x	M _y	M _z	
intact	2809.7	-2269.2	2404.2	80.8	131.0	-146.6	T _x
ACL cut	6844.2	-2180.9	3974.5	7.5	-91.2	-183.7	
intact		5999.5	-2814.8	-44.4	-233.3	-259.5	T _y
ACL cut		6825.3	-3309.0	14.7	-173.7	-497.3	
intact			5413.3	-38.9	-31.5	106.3	T _z
ACL cut			8286.1	-15.4	-85.7	29.4	
intact				6.1	7.7	-11.5	R _x
ACL cut		Symmetric		3.7	0.3	-3.6	
intact					25.3	-1.0	R _y
ACL cut					18.2	28.0	
intact						50.2	R _z
ACL cut						62.2	

Table 5

60° of F-E

Status of knee	F_x	F_y	F_z	M_x	M_y	M_z	
intact	1038.8	-2009.0	883.6	36.7	51.2	-19.6	T_x
ACL cut	7395.4	390.6	7797.7	14.4	-335.8	-469.8	
intact		4572.4	-614.6	-12.9	-70.6	-152.1	T_y
ACL cut		13138.0	-16450.8	80.1	-163.3	-403.5	
intact			6649.7	-129.9	-230.8	23.3	T_z
ACL cut			54978.5	-37.2	-217.4	-328.3	
intact				22.5	23.7	-37.3	R_x
ACL cut		Symmetric		33.2	10.9	-27.6	
intact					28.3	-35.1	R_y
ACL cut					38.6	11.3	
intact						81.5	R_z
ACL cut						64.2	

75° of F-E

Status of knee	F_x	F_y	F_z	M_x	M_y	M_z	
intact	4169.3	-3777.8	-605.7	9.7	26.8	107.9	T_x
ACL cut	1957.1	-2342.8	457.9	6.8	-7.9	30.4	
intact		3463.6	32.0	-0.1	-11.6	-99.6	T_y
ACL cut		2841.6	-579.5	4.9	-5.8	-89.2	
intact			6728.5	-104.2	-167.2	-20.3	T_z
ACL cut			7293.1	-68.4	-161.7	-44.8	
intact				3.3	3.8	-2.1	R_x
ACL cut		Symmetric		8.7	-2.5	-17.0	
intact					8.6	2.7	R_y
ACL cut					13.2	23.8	
intact						13.8	R_z
ACL cut						77.2	

90° of F-E

Status of knee	F_x	F_y	F_z	M_x	M_y	M_z	
intact	5369.0	-4264.1	84.9	-5.0	62.9	186.8	T_x
ACL cut	3212.3	-2740.7	123.7	5.9	-66.1	10.8	
intact		3668.6	-1475.8	18.5	-43.0	-156.1	T_y
ACL cut		2784.9	-1602.1	24.1	-35.7	-158.0	
intact			7038.5	-73.3	-40.4	35.5	T_z
ACL cut			8908.0	-60.5	-133.3	-45.3	
intact				1.9	1.5	0.4	R_x
ACL cut		Symmetric		7.5	-10.2	-14.3	
intact					10.7	11.0	R_y
ACL cut					70.1	92.1	
intact						15.5	R_z
ACL cut						126.1	

